Lowest excited 2^+ and 3^- states in even-A $N = 82$ and $N = 126$ isotones from relativistic quasiparticle random-phase approximation

A. Ansari
Institute of Physics, Bhubaneswar-751005, India

(Received 4 January 2017; revised manuscript received 10 March 2017; published 15 May 2017)

Excitation energy, reduced transition rates, and g factors of the lowest 2^+ and 3^- states of even-even $N = 82$ and $N = 126$ isotones are studied in relativistic QRPA formalism. These values are compared to available experimental data and some of the recent theoretical results. In the following the obtained results are presented first for $N = 82$ isotones with $Z = 36$–72, that is very neutron-rich to neutron-deficient nuclei with N/Z varying from 2.28 to 1.14 and then for $N = 126$ isotones with $Z = 76$–92. These calculations are performed employing NL3, as well as its recently revised version NL3* set of the RMF Lagrangian parameters. It is found that both the interaction sets produce almost similar results. The agreement with available data is rather satisfactory in view of such a wide range of nuclei considered here, though there are serious disagreements like in the case of ^{140}Ce and properties of 3^- states of $N = 126$ isotones.

DOI: 10.1103/PhysRevC.95.054309

I. INTRODUCTION

Since the early 1980s there have been attempts to study the structure of $N = 82$ isotones (for example, Refs. [1,2]). As early as 1971, Maier *et al.* [3] studied the excited levels of the $N = 126$ isotones with $Z = 85$–88 ($Z > 82$) by in-beam γ-ray spectroscopy with heavy ion reactions. However, for $Z < 82$ isotones the experimental information is even now very scarce. Some spectroscopic information for ^{206}Hg could be obtained only in 2001 [4] and for ^{204}Pt only in 2008 [5] and, as far I am aware, there are no data available for ^{202}Os. By now it is well known from light nuclei that for very neutron-rich nuclei nearing the neutron-drip line new magic numbers may appear or usual closed-shell energy gaps may get reduced (**quenched**). For the type of isotones considered here some recent studies [6–8] put forward arguments that for $Z < 50$ shell quenching should occur at $N = 82$. In a self-consistent mean-field calculation Dobaczewski *et al.* [6] demonstrated that for an isobar of $A = 120$ ($Z = 38$) the $N = 82$ shell gap decreases dramatically. Based on high Q_β value (8.34 MeV) for ^{130}Cd Dillmann *et al.* [7] believed that it is a direct signature of $N = 82$ shell quenching. Taprogge *et al.* [8] in their study of $2p_{3/2}$ proton-hole state in ^{132}Sn conclude that their study provided a robust evidence for the disappearance of the $Z = 38$ and 40 proton subshell closure at $N = 82$. As a consequence, a significant reduction of the $N = 82$ gap in the region of the r-process path for nucleosynthesis is expected. In fact, based on this observation the present study has been extended down to $Z = 36$.

However, Jungclaus *et al.* concluded in Ref. [9] that their observation of isomeric decays in ^{130}Cd and their interpretation in terms of shell-model calculations show no evidence of shell quenching at $N = 82$. That is, there is need to go down to even lighter $N = 82$ nuclei for their mass measurements and spectroscopic investigations. Similar conclusions were drawn by Watanabe *et al.* [10] in their study of isomers in ^{128}Pd ($Z = 46$).

Regarding shell quenching for $Z < 82$ in $N = 126$ nuclei, again a similar conclusion was drawn by Steer *et al.* [5] studying the isomeric decays in ^{204}Pt emphasizing the need for investigations towards $Z \leqslant 72$.

In view of these, and to further extend our earlier studies, I have undertaken to study the structure of 2^+ and 3^- excited states of these isotones in the relativistic quasiparticle random phase approximation (RQRPA) which has been quite successful for the description of tin and lead isotopic chains [11,12]. Here it may be useful to discuss briefly as to how successful has been the RQRPA predictions regarding the experimental data, say, on $B(E2; 0^+ \rightarrow 2^+)$ [in short $B(E2)\uparrow$] of the long chain of Sn isotopes before proceeding further to present and discuss the results on $N = 82$ and $N = 126$ isotones. In Fig. 1 for $A = 100$–134 tin isotopes the curve labeled "Expt-a" represents the experimental data [13] as reported a decade ago in Ref. [11] and that labeled "NL3" indicates the RQRPA predictions for the whole range of $N = 50$–84 isotopes with a shallow minimum at $N = 66$ (the midshell nucleus). For the stable isotopes $A = 112$–122 the agreement with experimental data (Expt-a) is quite poor, though for $A > 124$ it is very satisfactory. The shell-model results [14] are in good agreement for $A = 116$–130, predicting a symmetric distribution with a maximum at the midshell ($N = 66$). On the other hand, RQRPA predicted a very asymmetric distribution with a maximum at $A = 106$, a very neutron-deficient isotope. Recently, Doornenball *et al.* [15] emphasized that our predicted low values for **stable** isotopes triggered re-measurements of these isotopes, including extension to a lower mass region. As can be seen, the latest remeasured values for $A = 112$–124 (Expt-b), all are lowered relative to the earlier values. Thus, the latest values [15–19] are now in good agreement with the predictions done a decade ago, including the minimum at $N = 66$. In view of the above indicated

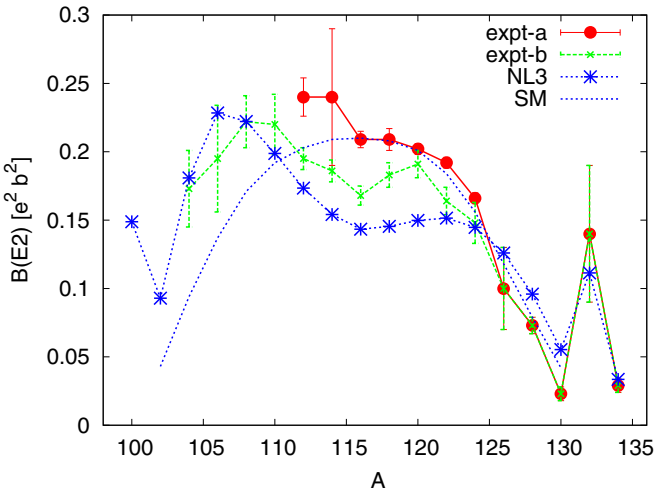

FIG. 1. Variation of $B(E2)\uparrow$ of tin isotopes with mass number A. Experimental data "Expt-a" represent the adopted values taken from [13] for $A = 112$–124 and from Ref. [16] for $A = 126$–134 (as reported in Ref. [11]). Expt-b indicates the latest values taken from Refs. [15–19]. The label NL3 indicates the RQRPA results [11] using the corresponding force parameters listed in Table 1. The shell model (SM) numbers are taken from Ref. [14].

success, the same scheme of calculation is employed here to study the structure of the $N = 82$ and $N = 126$ isotones.

II. CALCULATIONAL DETAILS

As far the calculational details, as discussed in Refs. [11,12], the full RQRPA formulation is presented in Ref. [20]. For the effective interaction the NL3 [21] and NL3* [22] parameter sets are used for the relativistic mean field (RMF) Lagrangian. The pairing part of the Gogny finite-range interaction D1S [23] is used as a phenomenological pairing interaction. For the basis space 20 or 16 harmonic oscillator shells are considered depending on the mass number along with hole-particle (or two quasiparticles) energy cutoff of 150 MeV, and that of hole-antiparticle energy cutoff of 1800 MeV (for details see Ref. [12]). The NL3 and NL3* parameter sets for the RMF Lagrangian are presented in Table I. The table also shows how well the nuclear matter properties are reproduced using these parameters, the main difference being seen on the values of the incompressibility parameter K and the symmetry energy J.

TABLE I. Parameter sets NL3 [21] and NL3* [22] of the effective forces used in the present calculation including the nucleon mass m.

Force parameters			Nuclear matter properties		
	NL3	NL3*		NL3	NL3*
m (MeV)	939.0	939.0	ρ_0 (fm^{-3})	0.148	0.150
m_σ (MeV)	508.194	502.5742	$(E/A)_\infty$ (MeV)	16.30	16.31
m_ω (MeV)	782.501	782.600	K (MeV)	271.76	258.27
m_ρ (MeV)	763.000	763.000	J (MeV)	37.4	38.68
g_σ	10.217	10.0944	m^*/m	0.60	0.594
g_ω	12.868	12.8065			
g_ρ	4.474	4.5748			
g_2 (fm^{-1})	−10.431	−10.8093			
g_3	−28.885	−30.1486			

III. RESULTS AND DISCUSSIONS

A. $N = 82$ isotones

It may be useful to present the RMF [relativistic Hartree-Bogoliubov(RHB)] results for all the isotones considered here to see how well the ground-state binding energies are reproduced. Out of 19 nuclei considered here only ^{132}Sn is included in the list of the spherical nuclei that are used for fitting these force parameters. The binding energy per particle (B/A), taken as positive, is listed for NL3 as well as NL3* along with the available experimental data [24] in Table II. Also shown are the pairing energy (in MeV) due to protons corresponding to the NL3 force. This last would be qualitatively indicative of the density of states near the Fermi surface, which have implications, at least, on the low-lying excitation properties. As can be seen, the B/A values are slightly higher for NL3 compared to that for NL3* till $A = 142$ and slightly lower for heavier ones. For most of the nuclei the calculated values show slight overbinding. To be specific it may be mentioned that for ^{132}Sn itself there is overbinding by about 1.0 MeV and that for ^{154}Hf it is about 3.7 MeV (≈2.4%). Another noticeable thing is the disappearance of the pairing energy for ^{140}Ce, which does not seem to be realistic as it is not known to be a doubly closed shell nucleus ($g_{7/2}$ subshell

TABLE II. Binding energy per particle B/A (in MeV) for $N = 82$ isotones calculated in RHB formalism with NL3 and NL3* set of the Lagrangian parameters. Expt denotes the experimental values taken from Ref. [24]. The last column shows the pairing energy (in MeV) due to protons.

Nucleus	B/A			E^P_{pair}
	NL3	NL3*	Expt	NL3
^{118}Kr	7.241	7.197		5.046
^{120}Sr	7.470	7.432		6.704
^{122}Zr	7.671	7.638		8.529
^{124}Mo	7.848	7.819		10.090
^{126}Ru	8.004	7.978		10.256
^{128}Pd	8.141	8.119	8.141	8.799
^{130}Cd	8.261	8.241	8.256	5.542
^{132}Sn	8.362	8.345	8.355	0.0
^{134}Te	8.396	8.381	8.384	4.280
^{136}Xe	8.414	8.403	8.396	5.921
^{138}Ba	8.418	8.409	8.393	5.175
^{140}Ce	8.407	8.400	8.376	0.0
^{142}Nd	8.370	8.367	8.346	7.249
^{144}Sm	8.321	8.321	8.304	11.074
^{146}Gd	8.262	8.265	8.250	13.720
^{148}Dy	8.194	8.198	8.181	15.522
^{150}Er	8.118	8.124	8.102	16.543
^{152}Yb	8.033	8.041	8.016	16.767
^{154}Hf	7.942	7.950	7.918	16.162

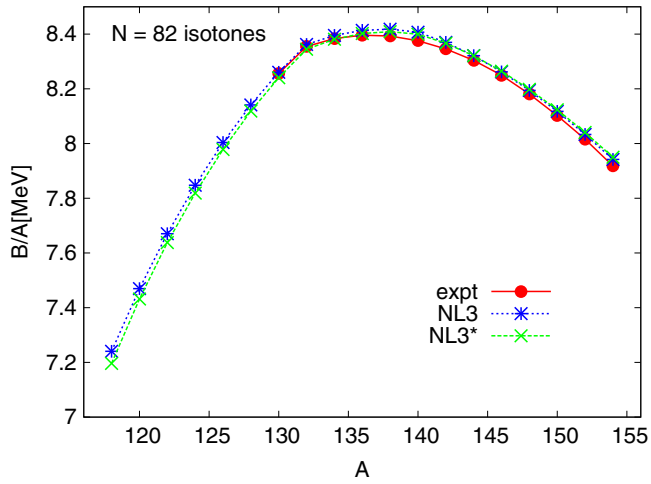

FIG. 2. Variation of binding energy per nucleon (B/A) with mass number A for $N = 82$ isotones. Experimental data are taken from Ref. [24].

closure with energy gap = 3.664 MeV). To highlight these differences in B/A values in a more visual manner these are displayed as a B/A versus A plot in Fig. 2.

In passing, it may be mentioned that the excitation energies are usually not so sensitive to the absolute value of the ground-state binding energy of a nucleus as compared to the single-particle levels in the vicinity the Fermi surface.

Now in Fig. 3 are presented the main results for the $J = 2^+$ excited states of ^{118}Kr to ^{154}Hf nuclei. The calculated numbers for E_2, $B(E2) \uparrow$ and g factor g_2 using NL3 as well as NL3* sets of the force parameters are compared to the available experimental data, and some of the other theoretical model results. An obvious result to be noticed is that the NL3 and NL3* sets produce almost similar results for all the three quantities shown here, except that for $A \leqslant 126$ the g_2 values obtained with NL3* are somewhat smaller than those with the NL3 set.

In Fig. 3(a) excitation energies E_2 are compared to the experimental data [25]. For $A \geqslant 132$ the agreement is satisfactory except for ^{140}Ce and ^{146}Gd. In fact, for $Z = 66$–72 the ageement is quite good. For $Z < 50$ the calculated numbers are higher with a small bump at $Z = 40$, as should be expected.

Other theoretical results are not displayed, as most of these calculations adjust the interaction parameters to reproduce these, at least for some of the nuclei in the considered mass range. However, it may still be useful to discuss briefly the findings of two recent theoretical calculations.

(i) Recently Terasaki, Engel, and Bertsch [26] performed QRPA calculations employing the Skyrme interaction SkM*. They made a very elaborate systematic study of the 2^+ excitation energy in 178 spherical nuclei. In the context of the present results for $N = 82$ isotones, even the excitation energies, E_2 are not as well reproduced as here in the RQRPA. Surprisingly, even they find at $Z = 58$ a shell closure effect with sudden increase in the E_2 value and for $Z > 58$ they obtain higher values compared to the experimental ones. Also

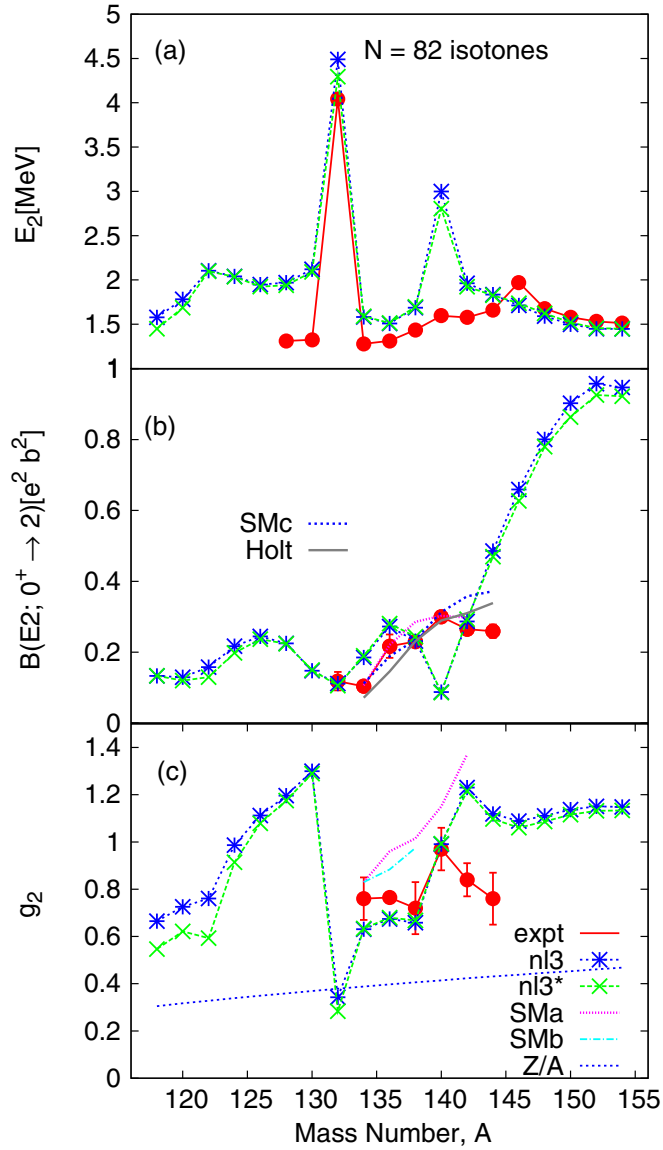

FIG. 3. Variation of E_2, $B(E2; 0 \rightarrow 2)$ and g factor g_2 as a function of mass number for $N = 82$ isotones. The labels Holt [2] and SMc [29] for $B(E2)$ and SMa [28], SMb [31] for g_2 represent shell model values and "expt" is the experimental data from Refs. [25,30].

at $Z = 64$ they do not obtain a rise as seen in the experimental data.

(ii) A generator coordinate method (GCM) calculation with particle number and angular momentum projected Hartree-Fock-Bogoliubov wave function using quadrupole deformation parameter as the generator coordinate was performed recently by Rodriguez *et al.* [27]. They studied the evolution of 2^+ excitation energies in a long chain of Cd isotopes for $N = 50$ to 82 employing the finite-range density-dependent Gogny interaction [23]. The trend of the variation of E_2 with N comes out quite well, but the calculated energies are higher by a couple of hundred keV throughout, so much so that at $N = 50$ and $N = 82$, respectively, the calculated values are about 1.0 and 2.0 MeV higher. In the present RQRPA calculation it comes to be higher by about 800 keV for ^{130}Cd.

The most important quantities sensitive to the single-particle structure near the Fermi level are the $B(E2)$ transition rates and the g factors. In Fig. 3(b) the $B(E2)\uparrow$ rates are displayed with experimental data available only for $Z = 50$–62 [25]. The RQRPA results are in quite close proximity to the experimental data except for ^{140}Ce and ^{144}Sm. However, a sharp drop of the values at $Z = 60$ and 62 relative to the value at $Z = 58$ is very significant, which none of the models including RQRPA is able to reproduce. For $B(E2)$ rates three shell-model curves are displayed indicated by SMa [28], SMc [29], and Holt [2]. In SMa the authors considered a so-called nucleon-pair approximation (NPA) of active protons in the–major shell, which includes the $1g_{7/2}, 2d_{5/2}, 2d_{3/2}, 3s_{1/2}, 1h_{11/2}$ orbitals for even-A $Z = 52$–60 nuclei. If all the possible pairs are considered, the NPA space is equivalent to the full shell-model space; if only a few important pairs are considered, it provides a truncated model space. This is the main theme of this scheme of calculations, the considered nuclei being ^{134}Te to ^{142}Nd. The employed two-body interaction is a model monopole and quadrupole pairing + quadrupole-quadrupole and octupole-octupole interaction between the valence protons. The effective charge for protons is 1.7 e. For such a limited number of nuclei the agreement with data are rather good, including a small drop for ^{142}Nd.

In SMc ^{144}Sm is also included within the same single-particle shell-model space as in SMa, but using a realistic effective Hamiltonian. The single-particle (sp) energies as well as the two-body effective interaction are derived from the high precision CD-Bonn potential with a cutoff momentum $\Lambda = 2.6\,\mathrm{fm}^{-1}$. Though the sp energies are not taken from experiments, these are computed adjusting this Λ to be close to the experimental values. Without discussing further on the model, it can be seen from the plot that the $B(E2)$ rates are only rising without any decrease after $A = 140$.

The third plot by Holt *et al.* [2] also shows only an increasing trend for the considered nuclei with $Z = 52$–62. Here also the spherical sp model space is the same $3s, 2d, 1g_{7/2}, 1h_{11/2}$ proton orbitals with energies taken from experimental spectrum of ^{133}Sb and for $2s_{1/2}$ from Sagawa *et al.* [1]. The effective two-body interaction is the G matrix derived from meson-exchange potential models. The proton effective charge is taken to be 1.4 e.

We may add that Sagawa *et al.* [1] also computed $B(E2)$ rates for even $Z = 52$–68 nuclei following shell model + core polarization and a generalized seniority scheme including core polarization. The effective Hamiltonian was determined by a least squares fit to the well-determined combination of two-body matrix elements to experimental energy-level data in the $A = 133$–148 region with the initial values calculated from a surface-delta parametrization. The shell-model results show a kink at ^{144}Sm similar to the experimental value, while the results of the generalized seniority scheme show a nearly linear increase.

Coming back to RQRPA, the curves (for NL3 and NL3* both) depicting a rapid increase of the $B(E2)$ values (for $A > 142$) appear rather surprising, which can be settled only when some experimental data are available for this mass region (very neutron-deficient). However, one point to be noted is that E_2 values for this region are small and gradually decreasing with the increase of Z, which is quite well reproduced by the RQRPA calculation. The predictions here for the lower mass region ($A < 132$) may also turn out to be important in view of expected quenching of the $N = 82$ shell gap with the decrease of Z values.

Before moving to the discussion on g factors it may be useful to make some comments on the results for ^{140}Ce. Since in the present calculation the proton pairing energy is coming out to be zero (see Table II), to see the effect of pairing, the calculation has been repeated increasing the pairing interaction strengh by 10% by multiplying all the pairing channel matrix elements of the Gogny-D1S interaction by a constant factor, $V_{\mathrm{fac}} = 1.10$ corresponding to the NL3 parameters. This leads to some improvement in the right direction with $E^P_{\mathrm{pair}} = 6.595$ MeV and $B/A = 8.412$ MeV. The values of E_2 and $B(E2)$ presented in Fig. 3 change to $E_2 = 2.910$ MeV (about 100.0 keV lower), and $B(E2)\uparrow = 0.275\ e^2\ b^2$ (about three-fold higher).

However, here one would not like to indulge much in such type of playing with parameters. Moreover, even if one finds some other force parameter set which is, say, good for ^{140}Ce and ^{146}Gd, there may not be any guarantee that it would be good for all other nuclei too. In such a scenario one option, though not quite desirable, may be to have more than one version of the NL3 (or some other) set, like several versions of Skyrme interactions in the nonrelativistic approach, by inclusion of the relevant spherical nuclei in a given mass region while fitting the force parameters.

Now coming to g factor values of these nuclei, Fig. 3(c) exhibits the RQRPA results along with experimental data [30] and some model calculations SMa [28] and SMb [31]. RQRPA results using NL3 set of parameter for $Z = 52$–70 have already appeared in Ref. [32] and compared to the available data for $Z = 54$–62. Now NL3* is also used for the calculation and the number of nuclei is extended further, particularly to lower Z values. The RQRPA results are in good agreement with the data for four nuclei, but are significantly higher for $Z = 60$ and 62, predicting almost a constant value for higher masses. After using $V_{\mathrm{fac}} = 1.10$ for ^{140}Ce the g_2 value has slightly decreased to 0.933 (compared to 0.991). The shell-model results show only an increasing trend besides the agreement at ^{134}Te. It is important to notice that the curve depicting Z/A values, a signature of collectivity, is far below the experimental as well as the theoretical points, except for ^{132}Sn which is due to a large negative contribution from neutrons.

To have some understanding of the contributions of the neutrons and protons to the physical quantities computed, in Fig. 4 is shown the contribution of neutrons I_n to the total QRPA wave-function normalization $I = 1$ for $J = 2^+$ as well as $J = 3^-$ for both the parameter sets. As can be seen the variation of I_n with A is almost similar for NL3 (upper panel) as well as NL3* (lower panel). Concentrating on the variation of I_n with A for $J = 2$, it may be noticed that at $Z = 50$ (^{132}Sn) the neutron contribution is almost 80%, the remaining 20% coming from protons. In the plot each point shows the summed up contributions from pairs of two quasiparticles or hole particles. As an illustration we list here the contribution to I_n from one hole-particle (or two quasiparticle) pair of $(1h_{11/2}, 2f_{7/2})$, nearest to the Fermi level, from $Z = 48$ down

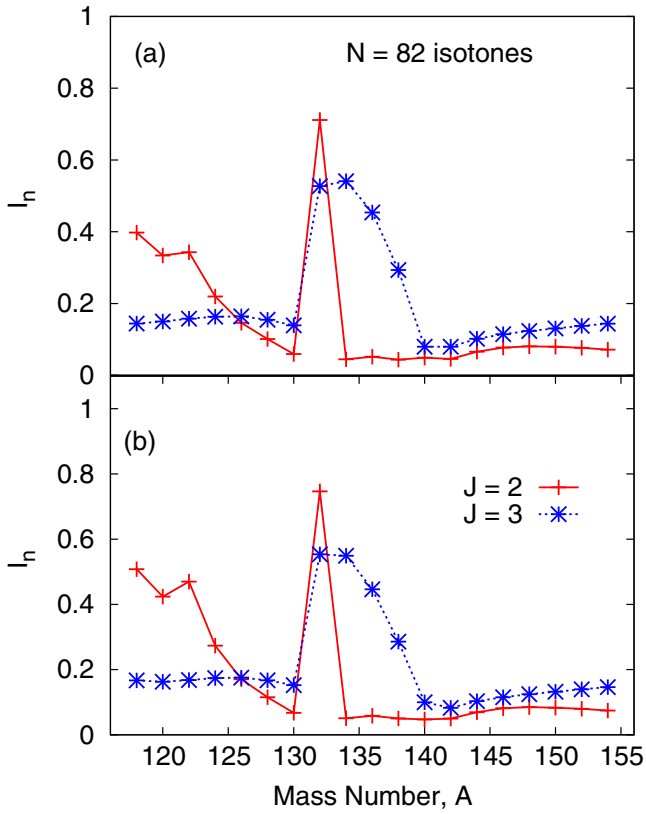

FIG. 4. Variation of the neutron contribution I_n to the total overlap I normalized to unity as a function of the mass number for $N = 82$ isotones. The upper panel (a) corresponds to the NL3 set of the parameters and the lower one to NL3*.

to 36: 0.038, 0.072, 0.108, 0.177, 0.297, 0.291, and 0.352. An increase in the value of I_n shows an increasing contribution of neutrons to the 2^+ excitation energy, $B(E2)$ and g_2 which is clearly reflected in their values in the previous figure. It may be a sign of quenching of the $N = 82$ shell gap as the proton number decreases. To look for quenching of the shell gap at $N = 82$ an RHB calculation was performed with a monopole pairing adjusting the interaction strength to reproduce almost the same pairing energy as obtained by the use of the Gogny interaction. The energy gap at $N = 82$ in ^{132}Sn is 6.314 MeV, i.e., between the sp states $2f_{7/2}$ and $1h_{11/2}$. This gap goes decreasing with the decrease of Z. For example, for ^{130}Cd, ^{128}Pd, ^{122}Zr, and ^{120}Sr the energy gaps (in MeV) at $N = 82$ are 5.817, 5.320, 3.910, and 3.665, respectively. Also it is found that there is no proton subshell closure at $Z = 38,40$ as discussed by the authors of Ref. [8]. In ^{120}Sr the energy gap between $2p_{3/2}$ and $2p_{1/2}$ levels is 1.224 MeV, whereas at $Z = 50$ the shell gap is 5.657 MeV.

As Fig. 4 shows, the contribution of neutrons to I_n is very small for $Z > 50$, and so the protons contribute more than 80% leading to a fast increase in the $B(E2)$ rates. The rise for g_2 is not so steep as it depends sensitively on the sp orbitals around the Fermi level. The variation of I_n for $J = 3^-$ will be discussed after presentation of the corresponding energy, transition rates and g factors in the next paragraph.

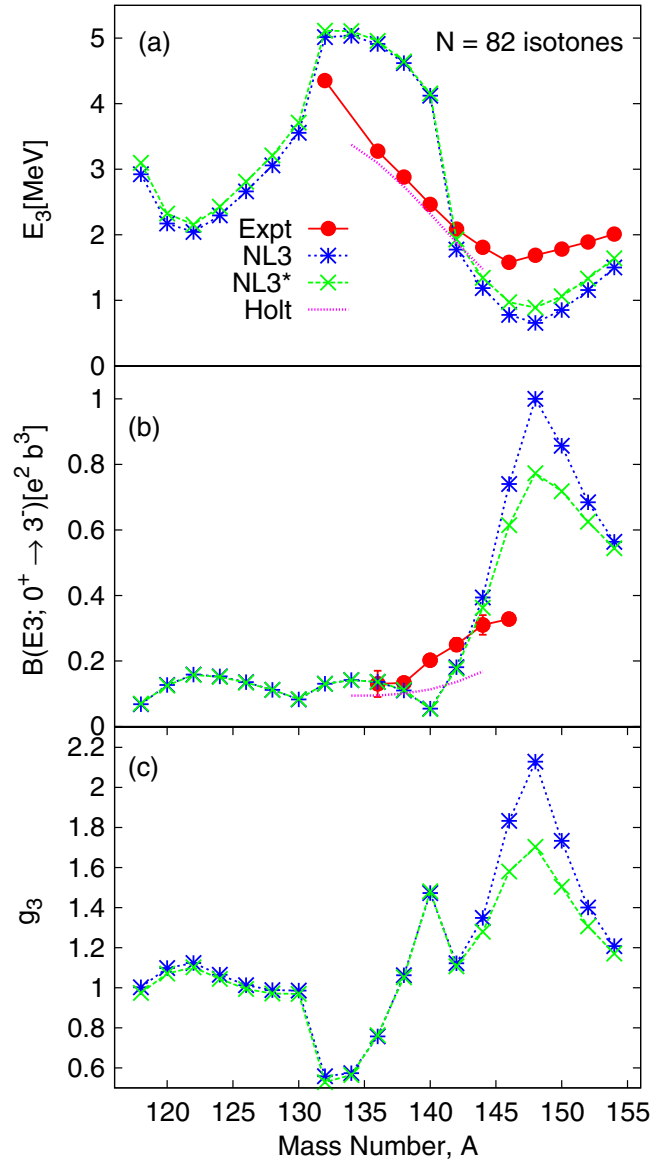

FIG. 5. Variation of E_{3^-}, $B(E3; 0 \rightarrow 3^-)$ and g factor g_3 as a function of mass number for $N = 82$ isotones. Experimental data taken from Ref. [33]. The label "Holt" indicates QRPA values of Holt *et al.* [2].

The results for the $J = 3^-$ states of the $N = 82$ isotones are presented in Fig. 5. Figure 5(a) shows the variation of E_{3^-} versus A. Qualitatively, the shape of the experimental curve [33] is reproduced with NL3 as well as NL3* parameters including a dip around ^{146}Gd and ^{148}Dy (proton midshell nucleus) contrary to the fact that for $J = 2^+$ the small hump at ^{146}Gd was not reproduced. However, quantitatively for most of the nuclei the computed numbers are quite off. The RQRPA calculation is predicting a similar shape and curvature in the lower mass region with a dip at $Z = 40$. The other theoretical curve presented is by Holt *et al.* [2] for $Z = 52$–62 in the QRPA approach, and for the limited number of nuclei considered by them the agreement with the experiment is really good.

Figure 5(b) displays the $B(E3) \uparrow$ results where the experimental data are known only for $Z = 54$–64. Except for ^{140}Ce

and ^{146}Gd, the RQRPA numbers are close to the experimental points for the other four nuclei. For the lower part, $Z \leqslant 50$, our numbers are $\leqslant 0.2\ e^2\ b^3$ which rise sharply for $Z > 60$ with a peak at $Z = 66$ (midshell number), where the NL3 and NL3* numbers are somewhat different from each other. It may be noticed that corresponding to dips in the E_3 curve there are peaks in the $B(E3)$ curve. The QRPA results of Holt *et al.* [2] in this case are not as close to experimental points as for E_{3^-}, but are still reasonably close.

As discussed above, with $V_{\rm fac} = 1.10$ for ^{140}Ce, the numbers improve in the right direction: $E_3 = 3.532$ MeV (about 600 keV lowered), $B(E3) = 0.106\ e^2\ b^3$ (almost doubled), $g_3 = 1.007$ (reduced compared to 1.473 otherwise, as can be seen below).

In Fig. 5(c) g_3 values are displayed(with $V_{\rm fac} = 1.0$). Unfortunately, there are no experimental or even theoretical results available to compare. Except for ^{140}Ce the numbers for other nuclei should be reliable, at least qualitatively. At $Z = 66$ here too NL3 and NL3* values of g_3 are not very close to each other. At $Z = 50$ and 52 the value of g_3 is the lowest as the neutrons contribute about 60% to the total QRPA wave function normalization (see Fig. 4).

To throw some further light on the quantities calculated for 3^- state one may look back at variation of I_n for $J = 3^-$ in Fig. 4. Except at $Z = 50$–56, it is almost constant with a magnitude less than 0.2. For $Z = 50$–56, it is 0.527, 0.541, 0.454, 0.293, respectively, the highest contribution coming from $(3s_{1/2}, 2f_{7/2})$, $(2d_{3/2}, 1h_{9/2})$, $(1h_{11/2}, 1i_{13/2})$ pairs, being 0.127, 0.123, 0.070, respectively. Beyond ^{140}Ce the $B(E3)$ rates are increasing with a maximum at ^{148}Dy. Though, the I_p remains almost constant, the number of protons keeps increasing, and contribution from some other high-l pairs like $(1h_{11/2}, 1i_{13/2})$ keeps increasing, the proton pair $(2d_{5/2}, 1h_{11/2})$ contributing maximum. Now in the next section the results for the $N = 126$ isotones are presented and discussed.

B. $N = 126$ isotones

Here the number of nuclei considered is rather small in view of quite scarce experimental information. As already mentioned, the considered nuclei are even-A with $Z = 76$–92; three nuclei below $Z = 82$ and five with $Z > 82$. Excitation energy for the lowest 2^+ state is known only for $Z = 78$–90, and $B(E2)$ transition rate only for ^{208}Pb and ^{210}Po. Information on 3^- excited states is even more scarce.

Like in Table II the binding energy per particle and the pairing energy (due to protons) are presented in Table III. As for $N = 82$ isotones, here too NL3 shows a slight overbinding compared to NL3* values, and both give a little overbinding compared to the experimental value. Regarding the pairing energy, it vanishes for $Z = 92$ due to a shell gap above $1h_{9/2}$ sp state. For a visual benefit these are also displayed in a B/A versus A plot in Fig. 6. The difference in theoretical and experimental values is clearly visible. Specifically for ^{208}Pb which is used in the fitting of the force parameters the binding energy reproduction is within about 1% and that for ^{216}Th it is within about 4%.

TABLE III. Same as in Table II, but for $N = 126$ isotones.

Nucleus	B/A			$E^P_{\rm pair}$
	NL3	NL3*	Expt	NL3
^{202}Os	7.845	7.834	7.842	12.130
^{204}Pt	7.865	7.857	7.860	8.206
^{206}Hg	7.877	7.872	7.869	3.283
^{208}Pb	7.878	7.876	7.867	0.0
^{210}Po	7.854	7.852	7.834	4.739
^{212}Rn	7.822	7.822	7.795	6.987
^{214}Ra	7.784	7.786	7.749	7.375
^{216}Th	7.740	7.743	7.698	5.824
^{218}U	7.689	7.692	7.641	0.0

Like for ^{140}Ce, if $V_{\rm fac} = 1.10$ is used for ^{218}U then the proton pairing energy becomes 9.343 MeV and $B/A = 7.691$ MeV.

In the Fig. 7 are displayed the results for E_2, $B(E2)\uparrow$ and g_2 of the $N = 126$ isotones. In Fig. 7(a) the RQRPA calculated energies are in reasonably good agreement with the data for $A = 208$–216. For ^{218}U the computed value is very high, reflecting the subshell closure at $Z = 92$ which may not be realistic. However, with $V_{\rm fac} = 1.10$ it becomes 2.977 MeV, lowered by about 500 keV. The curve for $A = 202$–206 is flat at $\approx$2.0 MeV, about an MeV higher than the experimental value for ^{204}Pt.

In Fig. 7(b) the $B(E2)$ rates are displayed as a function of A which vary in an oscillatory manner. As reported awhile ago [12], there is good agreement with data for ^{208}Pb, but the steep drop at $Z = 84$ in the experimental value seems a puzzle. Considering ^{208}Pb as an inert core there are two protons in $1h_{9/2}$ orbitals, which should lead to a reasonably large transition quadrupole moment. The calculated number shows a slight rise for ^{210}Po. When the E_2 significantly drops relative to ^{208}Pb, the drop in $B(E2)$ as well seems very unusual. Another point to be noted is that E_2 is changing very linearly from $Z = 84$–90, whereas the calculated $B(E2)\uparrow$ values show an inverted parabola type variation. However, if $V_{\rm fac} = 1.10$

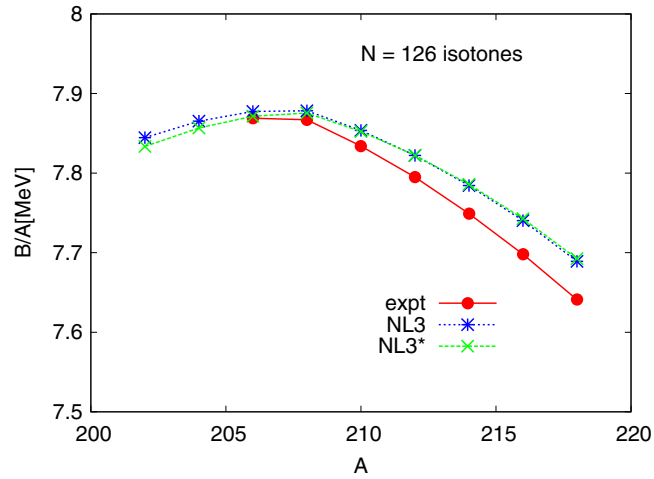

FIG. 6. Same as Fig. 2 for $N = 126$ isotones. Experimental data taken from Ref. [24].

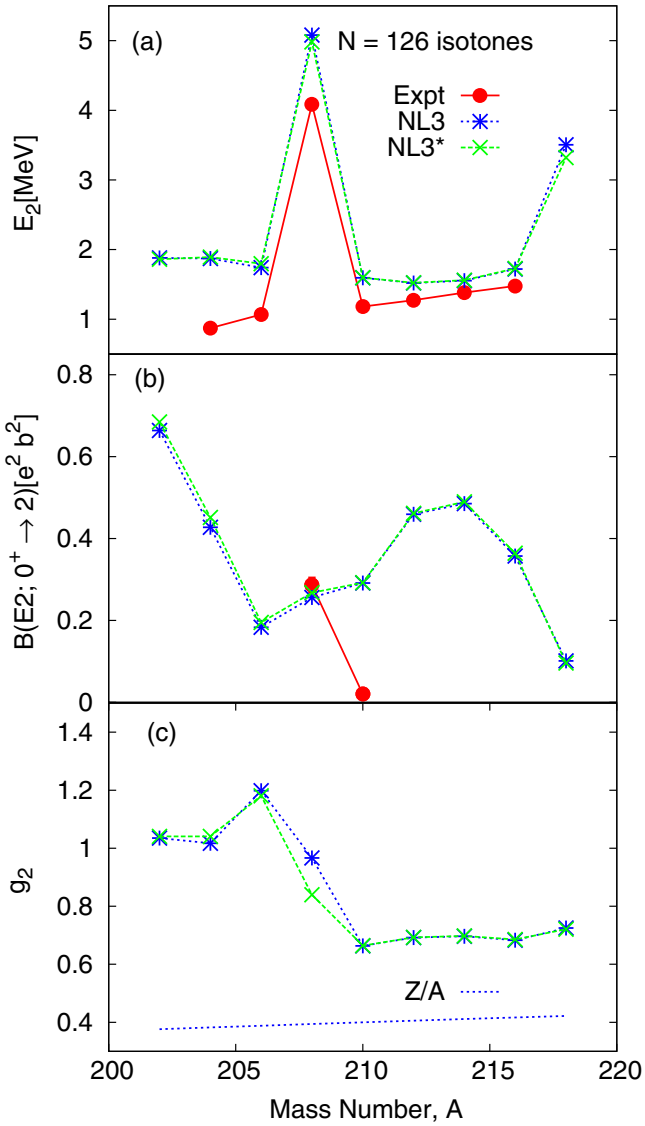

FIG. 7. Same as Fig. 3 for $N = 126$ isotones. Experimental data taken from Ref. [25].

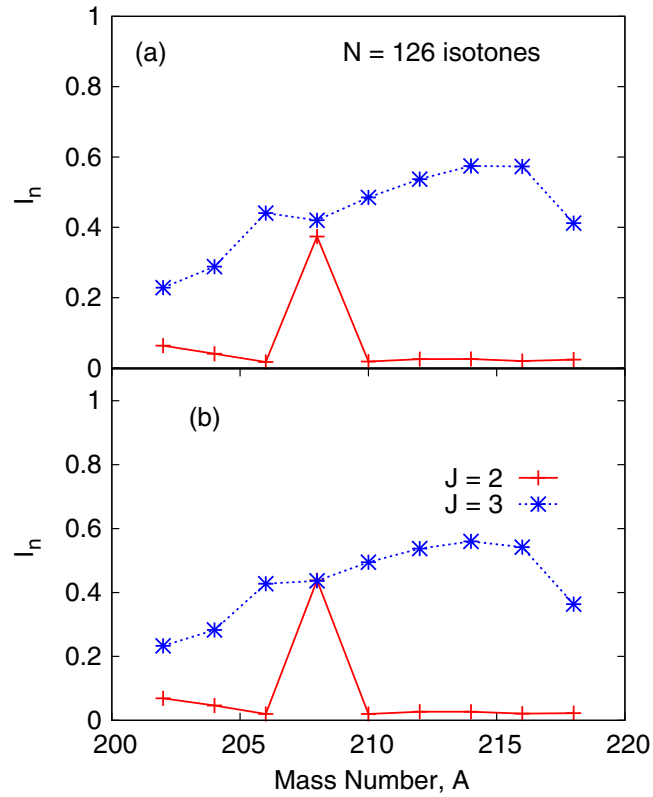

FIG. 8. Same as Fig. 4 for $N = 126$ isotones.

is used for ^{218}U the $B(E2)$ value increases almost five-fold to 0.575 $e^2\ b^2$.

The variation of g_2 with A is shown in Fig. 7(c) with no experimental or theoretical data available with which to compare. The Z/A curve is far below these RQRPA values. The sudden drop of g_2 from $A = 206$ to 210 indicates a sudden change in the single-particle structure around the Fermi level. For ^{218}U here again the value of g_2 changes in the presence of pairing to 0.880 with an increase of about 20%. It seems difficult to understand the behavior of $B(E2)$ and g_2 in terms of the variation of I_n with A (see Fig. 8). Except for ^{208}Pb the contribution of neutrons for $J = 2$ is negligible. For $Z < 80$ there is only a slight tendency of increase with the decrease of Z. So, first of all there seems no shell quenching at $N = 126$ (see the discussions in Ref. [5]). The value of $B(E2)$ is increasing in going down from ^{206}Hg to ^{202}Os, whereas the contribution of protons to the total QRPA wave function normalization ($I = 1$), I_p shows conversely a slight decreasing trend with values as 0.983, 0.959, and 0.937, respectively. Looking at the contribution to I_p of some of the two quasiparticle pairs, like $(1h_{11/2}, 1h_{11/2})$ and $(2d_{5/2}, 2d_{3/2})$ it is found that these go on increasing from Hg to Os. The former pair gives 0.012, 0.096, 0.258 and the latter gives 0.006, 0.032, 0.057, respectively. The quadrupole matrix elements of high-l pairs should be larger than those of the low-l pairs and this may explain the rise of $B(E2)$. A more detailed analysis is difficult in such a large basis of states and complex involved calculations in a transformed canonical basis.

Regarding some understanding of the dependence of g_2 on A, one may look at some two quasiparticle states near the Fermi level (smallest quasiparticle energy). For Po to Th when I_p is about 98% the value of I_p from a single quasiparticle pair $(1h_{11/2}, 1h_{9/2})$ is about 95%, thereby explaining the almost same value of g_2 for all of these nuclei. For the lighter mass nuclei three to four pairs contribute with some varying degrees: $(2d_{3/2}, 3s_{1/2})$, $(2d_{5/2}, 3s_{1/2})$, $(1h_{11/2}, 1h_{11/2})$, and so on.

Finally, in Fig. 9 is displayed the variation of E_3, $B(E3)$ and g_3 for $J = 3^-$ states of these nuclei on which experimental data available are only a few. Also, for $J = 3^-$ no other recent theoretical result seems to be available. As the figure shows, in Fig. 9(a) is displayed the variation of E_{3^-} with A. Experimental information is available only for Pb, Po, and Th. While the agreement with Pb is good, it looks totally off for the other two nuclei. Corresponding to NL3 and NL3* forces the numbers show some differences beyond ^{206}Hg.

In Fig. 9(b) the variation of $B(E3)$ transition rates versus A is shown which looks like an inverted parabola from $A = 204$

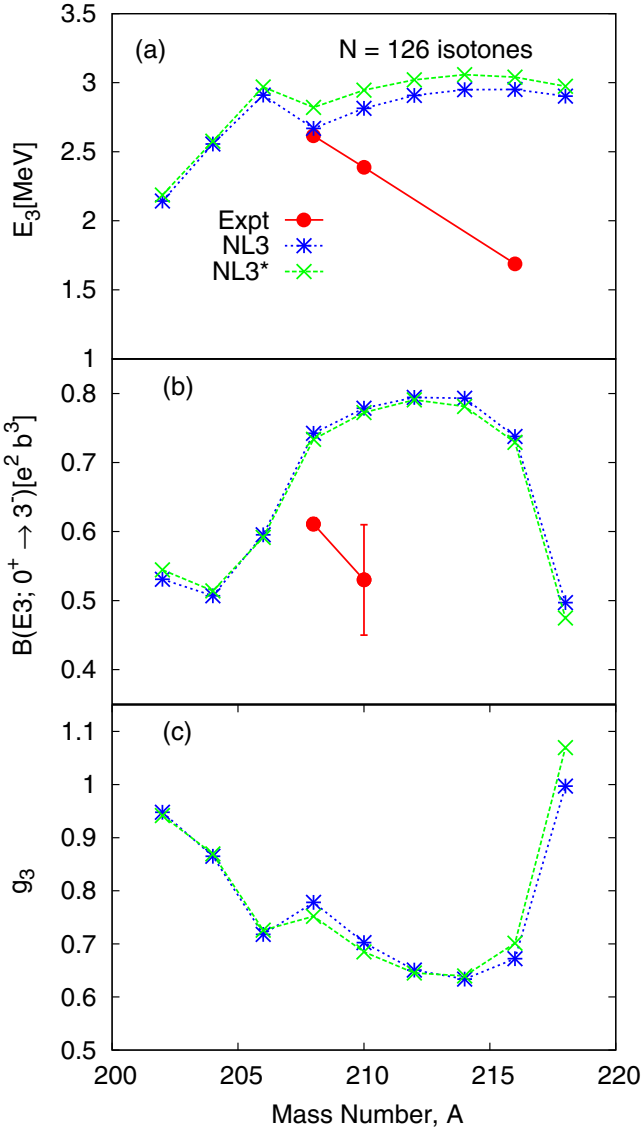

FIG. 9. Same as Fig. 5 for $N = 126$ isotones.

to 218, with a maximum at around ^{212}Rn (orbital $1h_{9/2}$ half filled). The values for ^{202}Os and ^{204}Pt are almost the same. The agreement with only two experimental points for ^{208}Pb and ^{210}Po is not so bad (higher by about 0.1 unit of $e^2\,b^3$) keeping in mind that there is no freedom to play with any parameter. Another way to look at is that it is almost a constant varying between 0.75 to 0.80 units for $A = 208$–216 with a sudden drop at $A = 218$. The I_p decreases almost linearly from 0.77 at $A = 202$ to 0.42 at $A = 208$, but $B(E3)$ shows jump. So, as Z increases and the proton Fermi level goes up the contribution from high-l two quasiparticles increases for I_p like: $(2d_{3/2},h_{9/2})$, $(1h_{11/},1i_{13/2})$, $(1h_{9/2},1i_{13/2})$, and so on. This should be the reason for the increase of these $B(E3)$ rates.

The curve showing the variation of g_3 in Fig. 9(c) looks almost like a mirror image of the $B(E3)$ plot above. Again as Fig. 8 shows, due to the increasing role of the neutrons with the increase of Z the g factor shows a decrease except at the two ends with the lowest and highest Z values. Certainly it cannot just be a smooth function of I_n or I_p, it has to depend on the sp levels near the Fermi surface including that of neutrons.

Again in the presence of nonzero pairing with $V_{\rm fac} = 1.10$ the values for the 3^- state of ^{218}U get changed to the following numbers: $E_3 = 2.437$ MeV (about 500 keV decrease), $B(E3) = 0.8368\ e^2\ b^3$ (about 70% increase), and $g_3 = 0.803$ (a decrease by about 20%).

IV. CONCLUSION

Excitation energies, reduced transition rates, and g factors of lowest 2^+ and 3^- states of several even-even $N = 82$ and $N = 126$ isotones were studied following RQRPA formalism for spherical nuclei. These calculations are performed employing the well-known NL3, as well as its recently revised version NL3* set of the RMF Lagrangian parameters. In all, 28 nuclei for two angular momentum cases were considered and it turns out that the use of NL3* shows hardly any significant difference on the values that were obtained with the use of the original version.

As far as $N = 82$ isotones are concerned, the experimental data on $B(E2)$, $B(E3)$, g_2, and g_3 are limited only to some nuclei in the $Z = 50$–64 region.

In view of there being no free adjustable parameter, the RQRPA numbers are over all in reasonable agreement with these data, with exceptions at $Z = 58$, 62 for $B(E2)$, $Z = 60$, 62 for g_2 and $Z = 58$, 64 for $B(E3)$. In the case of ^{140}Ce a good improvement is obtained if the pairing interaction strength is increased by about 10%. Furthermore, it may be noted that there is no other theoretical model calculation that reproduces these properties in a better agreement than what is obtained here.

The experimental data for $N = 126$ isotones are even more scarce. Out of the nine nuclei considered here, E_2 excitation energies are known for seven nuclei, and $B(E2)$ transition rates are available only for two, ^{208}Pb and ^{210}Po and none for g factors. The excitation energies for $Z \geqslant 82$ are well reproduced in RQRPA, though for ^{204}Pt and ^{206}Hg the agreement is not as good. The $B(E2)$ value for ^{208}Pb is in good agreement, but the case of ^{210}Po seems quite puzzling. The situation with E_{3^-} and $B(E3)$ is still worse as far as the experimental information is concerned.

A simultaneous reproduction of spectroscopic properties of 2^+ as well as 3^- states of these nuclei seems to be a very challenging task. Thus, there is a need for more efforts on experimental measurements as well as theoretical calculations.

Another aspect discussed above has been the quenching of $N = 82$ and $N = 126$ shell gaps for very neutron-rich nuclei. The present calculation seems to support the idea of shell quenching at $N = 82$ for $Z < 44$. On the other hand, this does not seem to be the case at $N = 126$.

ACKNOWLEDGMENTS

The RQRPA computer code was developed in collaboration with Peter Ring during the author's a few short visits to Technical University of Munich, Munich. I thank Dr. Ring for the hospitality and past collaboration.

[1] H. Sagawa, O. Scholten, B. A. Brown, and B. H. Wildenthal, Nucl. Phys. A **462**, 1 (1987).
[2] A. Holt *et al.*, Nucl. Phys. A **618**, 107 (1997).
[3] K. H. Maier, J. Phys. Colloque C **6**, 221 (1971).
[4] B. Fornal, R. Broda, K. H. Maier, J. Wrzesiński, G. J. Lane, M. Cromaz, A. O. Macchiavelli, R. M. Clark, K. Vetter, A. P. Byrne, G. D. Dracoulis, M. P. Carpenter, R. V. F. Janssens, I. Wiedenhoever, M. Rejmund, and J. Blomqvist, Phys. Rev. Lett. **87**, 212501 (2001).
[5] S. J. Steer *et al.*, Phys. Rev. C **78**, 061302(R) (2008).
[6] J. Dobaczewski, I. Hamamoto, W. Nazarewicz, and J. A. Sheikh, Phys. Rev. Lett. **72**, 981 (1994).
[7] I. Dillmann, K. L. Kratz, A. Wöhr, O. Arndt, B. A. Brown, P. Hoff, M. Hjorth-Jensen, U. Köster, A. N. Ostrowski, B. Pfeiffer, D. Seweryniak, J. Shergur, and W. B. Walters (the ISOLDE Collaboration), Phys. Rev. Lett. **91**, 162503 (2003).
[8] J. Taprogge *et al.*, Phys. Rev. Lett. **112**, 132501 (2014).
[9] A. Jungclaus *et al.*, Phys. Rev. Lett. **99**, 132501 (2007).
[10] H. Watanabe *et al.*, Phys. Rev. Lett. **111**, 152501 (2013).
[11] A. Ansari, Phys. Lett. B **623**, 37 (2005).
[12] A. Ansari and P. Ring, Phys. Rev. C **74**, 054313 (2006).
[13] S. Raman, C. W. Nestor, Jr., and P. Tikkanen, At. Data Nucl. Data Tables **78**, 1 (2000).
[14] A. Banu, J. Gerl, C. Fahlander, M. Gorska, H. Grawe, T. R. Saito, H. J. Wollersheim, E. Caurier, T. Engeland, A. Gniady, M. Hjorth-Jensen, F. Nowacki, T. Beck, F. Becker, P. Bednarczyk, M. A. Bentley, A. Burger, F. Cristancho, G. deAngelis, Z. Dombradi, P. Doornenbal, H. Geissel, J. Grebosz, G. Hammond, M. Hellstrom, J. Jolie, I. Kojouharov, N. Kurz, R. Lozeva, S. Mandal, N. Marginean, S. Muralithar, J. Nyberg, J. Pochodzalla, W. Prokopowicz, P. Reiter, D. Rudolph, C. Rusu, N. Saito, H. Schaffner, D. Sohler, H. Weick, C. Wheldon, and M. Winkler, Phys. Rev. C **72**, 061305(R) (2005).
[15] P. Doornenbal *et al.*, Phys. Rev. C **90**, 061302(R) (2014).
[16] D. C. Radford *et al.*, Nucl. Phys. A **746**, 83 (2004).
[17] A. Ekström, J. Cederkall, C. Fahlander, M. Hjorth-Jensen, F. Ames, P. A. Butler, T. Davinson, J. Eberth, F. Fincke, A. Gorgen, M. Gorska, D. Habs, A. M. Hurst, M. Huyse, O. Ivanov, J. Iwanicki, O. Kester, U. Koster, B. A. Marsh, J. Mierzejewski, P. Reiter, H. Scheit, D. Schwalm, S. Siem, G. Sletten, I. Stefanescu, G. M. Tveten, J. VandeWalle, P. Van Duppen, D. Voulot, N. Warr, D. Weisshaar, F. Wenander, and M. Zielinska, Phys. Rev. Lett. **101**, 012502 (2008).
[18] J. Cederkäll, A. Ekstrom, C. Fahlander, A. M. Hurst, M. Hjorth-Jensen, F. Ames, A. Banu, P. A. Butler, T. Davinson, U. DattaPramanik, J. Eberth, S. Franchoo, G. Georgiev, M. Gorska, D. Habs, M. Huyse, O. Ivanov, J. Iwanicki, O. Kester, U. Koster, B. A. Marsh, O. Niedermaier, T. Nilsson, P. Reiter, H. Scheit, D. Schwalm, T. Sieber, G. Sletten, I. Stefanescu, J. vandeWalle, P. vanDuppen, N. Warr, D. Weisshaar, and F. Wenander, Phys. Rev. Lett. **98**, 172501 (2007).
[19] A. Jungclaus *et al.*, Phys. Lett. B **695**, 110 (2011).
[20] N. Paar, P. Ring, T. Niksic, and D. Vretenar, Phys. Rev. C **67**, 034312 (2003).
[21] G. A. Lalazissis, J. Konig, and P. Ring, Phys. Rev. C **55**, 540 (1997).
[22] G. A. Lalazissis *et al.*, Phys. Lett. B **671**, 36 (2009).
[23] J. F. Berger *et al.*, Comput. Phys. Commun. **63**, 365 (1991).
[24] M. Wang *et al.*, Chin. Phys. C **36**, 1603 (2012).
[25] B. Pritychenko, M. Birch, B. Singh, and M. Horoi, At. Data Nucl. Data Tables **107**, 1 (2016).
[26] J. Terasaki, J. Engel, and G. F. Bertsch, Phys. Rev. C **78**, 044311 (2008).
[27] T. R. Rodriguez, J. L. Egido, and A. Jungclaus, Phys. Lett. B **668**, 410 (2008).
[28] Y. Y. Cheng, Y. M. Zhao, and A. Arima, Phys. Rev. C **94**, 024307 (2016).
[29] L. Coraggio, A. Covello, A. Gargano, N. Itaco, and T. T. S. Kuo, Phys. Rev. C **80**, 044320 (2009).
[30] N. J. Stone, At. Data Nucl. Data Tables **90**, 75 (2005).
[31] B. A. Brown, N. J. Stone, J. R. Stone, I. S. Towner, and M. Hjorth-Jensen, Phys. Rev. C **71**, 044317 (2005).
[32] A. Ansari and P. Ring, Phys. Lett. B **649**, 128 (2007).
[33] T. Kibedi and R. H. Spear, At. Data Nucl. Data Tables **80**, 35 (2002).